Assessment of Linear and Nonlinear Synchronization Measures for Analyzing EEG in a Mild Epileptic Paradigm

Vangelis Sakkalis, Ciprian Doru Giurcăneanu, *Member, IEEE*, Petros Xanthopoulos, Michalis E. Zervakis, *Member, IEEE*, Vassilis Tsiaras, Yinghua Yang, Eleni Karakonstantaki, and Sifis Micheloyannis

***Abstract*—Epilepsy is one of the most common brain disorders and may result in brain dysfunction and cognitive disturbances. Epileptic seizures usually begin in childhood without being accommodated by brain damage and are tolerated by drugs that produce no brain dysfunction. In this study, cognitive function is evaluated in children with mild epileptic seizures controlled with common antiepileptic drugs. Under this prism, we propose a concise technical framework of combining and validating both linear and nonlinear methods to efficiently evaluate (in terms of synchronization) neurophysiological activity during a visual cognitive task consisting of fractal pattern observation. We investigate six measures of quantifying synchronous oscillatory activity based on different underlying assumptions. These measures include the coherence computed with the traditional formula and an alternative evaluation of it that relies on autoregressive models, an information theoretic measure known as minimum description length, a robust phase coupling measure known as phase-locking value, a reliable way of assessing generalized synchronization in state–space and an unbiased alternative called synchronization likelihood. Assessment is performed in three stages; initially, the nonlinear methods are validated on coupled nonlinear oscillators under increasing noise interference; second, surrogate data testing is performed to assess the possible nonlinear channel interdependencies of the acquired EEGs by comparing the synchronization indexes under the null hypothesis of stationary, linear dynamics; and finally, synchronization on the actual data is measured. The results on the actual data suggest that there is a significant difference between normal controls and epileptics, mostly apparent in occipital–parietal lobes during fractal observation tests.**

Manuscript received October 17, 2007. Current version published July 6, 2009. This work was supported in part by the EC IST Project BIOPATTERN under Contract 508803. The work of C. D. Giurcăneanu was supported by the Academy of Finland under Project 113572, Project 118355, and Project 213462. The work of Y. Yang was supported by the Academy of Finland under Project 213462.

V. Sakkalis is with the Institute of Computer Science, Foundation for Research and Technology, Heraklion 71110, Greece. He is also with the Department of Electronic and Computer Engineering, Technical University of Crete, Chania 73100, Greece (e-mail: sakkalis@ics.forth.gr).

C. D. Giurcăneanu is with the Department of Signal Processing, Tampere University of Technology, Tampere 33720, Finland (e-mail: ciprian.giurcaneanu@tut.fi).

P. Xanthopoulos is with the Industrial and Systems Engineering Department, University of Florida, Gainesville, FL 32611 USA (e-mail: petrosx@ufl.edu).

M. E. Zervakis is with the Department of Electronic and Computer Engineering, Technical University of Crete, Chania 73100, Greece (e-mail: michalis@systems.tuc.gr).

V. Tsiaras is with the Department of Computer Science, University of Crete, Heraklion 71409, Greece (e-mail: tsiaras@ics.forth.gr).

Y. Yang was with the Department of Signal Processing, Tampere University of Technology, Tampere 33101, Finland. He is now with the Nokia Devices R&D, Tampere 33101, Finland (e-mail: yinghua.yang@tut.fi).

E. Karakonstantaki and S. Micheloyannis are with the Clinical Neurophysiology Laboratory (L. Widen), Faculty of Medicine, University of Crete, Heraklion 71409, Greece (e-mail: ekarakonstantaki@yahoo.gr; michelogj@med.uoc.gr).

Digital Object Identifier 10.1109/TITB.2008.923141

***Index Terms*—Brain, coupling, EEG, epilepsy, fractal patterns, nonlinear analysis, surrogate data, synchronization.**

I. Introduction

NEURONAL dynamics and synchronization phenomena have been increasingly recognized to be important mechanisms by which specialized cortical and subcortical regions integrate their activity to form distributed neuronal assemblies that function in a cooperative manner [1]. Synchronous oscillations of certain types of such assemblies in different frequency bands relate to different perceptual, motor, or cognitive states and may be indicative of a wider range of cognitive functions or brain pathologies [2], [3]. In general, low frequencies, like the theta band (4–8 Hz), are believed to reveal the coupling between distant brain regions, whereas high frequencies, like the gamma band (>40 Hz), are thought to be more important for short-range interactions [4].

The traditionally formulated but still the most common way of analyzing the functional coupling of cortical assemblies has been the *magnitude squared coherence* (MSC) or simply coherence. MSC is a normalized measure of linear dependence between two signals and is capable of identifying linear synchrony on certain frequency bands [5], [6], but it is not able to provide indications on the feedback that exists between the analyzed systems. To evaluate the causality between EEG channels, we resort to the measures derived in [7] from the *minimum description length* (MDL) principle. Since all the measures mentioned earlier are linear, we extend our investigations by also considering nonlinear measures. *Phase synchronization* (PS) presents a different approach in analyzing the possible nonlinear interdependencies of the EEG signal and focuses on the phases of the signals. The idea of studying the phase relationships of two neurophysiological signals is not new [8], but later studies have shown that even if the amplitudes of two coupled chaotic oscillators remain uncorrelated, their phases may synchronize [9]. A robust phase coupling measure is the *phase-locking value* (PLV) [10]. Finally, another group of synchronization measures is based on the assumption that neurons are highly nonlinear devices, which in some cases show chaotic behavior [11]. Hence, the use of nonlinear measures derived from studying chaotic dynamical systems may be of interest in neurophysiology applications. Such measures belong to the *generalized synchronization* (GS) concept and are based on analyzing the interdependence between the amplitudes of the

1089-7771/$25.00 © 2009 IEEE

signals in a state–space reconstructed domain. In this study, we use two variants of this idea, a *robust synchronization* (RS) measure proposed by [12], [13] and the *synchronization likelihood* (SL) method [14].

In this paper, we employ the aforementioned concepts toward investigating the capabilities of both linear and nonlinear measures in revealing the coupling between EEG channels in real band-limited signals. We decided to study a real case scenario in a group of children with mild types of seizures, either new onset or controlled, since they do not show any differences through clinical/psychological consideration, visual EEG inspection or traditional spectral analysis. Hence, we address the question of whether controlled-epileptic children exhibit synchronization differences in their EEGs in comparison to an age-matched control group during the performance of a control and a mental task. Most discrepancies between the EEGs of epileptic subjects as compared to controls have been studied in adults, and literature work that applies the traditional techniques for detecting epilepsy in children is rather conflicting [15]–[17]. Nevertheless, it is quite important to develop methods for evaluating the EEGs of children with some epileptic seizures in the past, but without neuropsychological or school disturbances, so as to assign an early course of treatment and reevaluation.

II. Methods

A. Artificial Signals and Real Data Acquisition

To study the robustness of each of the proposed nonlinear methods, we consider two artificially generated test signals by classical coupled chaotic dynamical systems. The first model uses two coupled Rössler oscillators, whereas the second uses a Lorenz system nonlinearly driven by a Rössler oscillator with such coupling coefficient that ensures GS [18], [19].

To study the real case clinical scenario, we analyzed a population that initially consisted of 21 children with epileptic seizures (common childhood epileptic seizures mainly "Rolandic type," idiopathic generalized seizures, focal secondary generalized seizures without detectable brain damage and absence seizures). These subjects were retrospectively selected from the pool of Pediatric Neurology outpatient Clinics of two hospitals in Heraklion, Crete, where they were diagnosed and regularly followed. Their diagnosis was based on clinical and EEG criteria of International League Against Epilepsy (ILAE). Six children had their first seizure episode 1–30 days (mean: 12.5 days), prior to their recruitment in the study. Sixteen children, previously diagnosed, entered the study, within 1–9 years (mean 4.2 years) after their seizure onset. All children were treated with the appropriate antiepileptic medication (in small doses without clinical side effects) and were well controlled. The control group included 21 volunteers, matched with the patient group for age, sex, area of residence, and parents' education. Inclusion criteria for patients and controls consisted of: 1) age of 9–13 years old, 2) normal intellectual potential [assessed with Wechsler Intelligence Scale for Children (WISC-III)], 3) absence of neurological damage documented by neurological evaluation for patients and controls and additionally by brain computed tomography (CT) and/or MRI scan for patients and parental interview for controls, and 4) absence of psychiatric problems (based on parent's interview). Two children were excluded from the final sample: one control and one epileptic child, for noncooperativeness and suspicion of psychiatric problems with brain damage, respectively. The final sample consisted of 20 children with seizures (11 girls, 9 boys) and 20 controls (11 girls, 9 boys). Patients and controls, all right handed, were individually evaluated in the Clinical Neurophysiology Laboratory, at the Medical School of the University of Crete. The parents of children participating in this study signed a written consent form, after having been informed about the study's purpose and the required procedures. The study was approved by the Local Ethics Committee.

The EEG signals in both groups (controls and epileptics) were recorded from 30 cap electrodes (FP1, FP2, F7, F3, FZ, F4, F8, FT7, FC3, FCZ, FC4, FT8, T3, C3, CZ, C4, T4, TP7, CP3, CPZ, CP4, TP8, P3, PZ, P4, P7, P8, O1, OZ, and O2), according to the 10/20 international system, referred to linked A1+A2 electrodes. The signals were amplified using a set of Contact Precision Instrument amplifiers, filtered online with a bandpass between 0.1 and 200 Hz, and digitized at 400 Hz. Offline, the recorded data were carefully reviewed for technical and biogenic artifacts by our clinical neurophysiology expert, so that only a single epoch of 10.24 s duration (4096 samples) as a representative for each subject was investigated.

B. Test Description

Continuous EEGs were recorded in an electrically shielded room, sound and light attenuated, while participants sat in a reclined chair. We analyzed epochs at rest, i.e., while each individual had the eyes fixed on a small point on the computer screen and during a visual cognitive task. The visual task involves fractal observation, which is typically used for the study of the psychology of perception [20]. This is because fractals are abstract visual targets that permit elimination of the effect of recognition and related side effects (like hidden associations and confounded conditions), which are difficult to control in the course of an experiment. Stimuli were presented on a liquid crystal display (LCD) screen located in front of the participants. Vertical and horizontal eye movements and blinks were monitored through a bipolar montage from the supraorbital ridge and the lateral canthus.

C. Magnitude Squared and Autoregressive (AR) Coherence (AR-COH)

Consider two simultaneously measured discrete-time series x_n and y_n, $n = 1,\ldots,N$. The most commonly used linear synchronization method is the cross-correlation function (C_{xy}) defined as

$$C_{xy}(\tau) = \frac{1}{N-\tau}\sum_{i=1}^{N-\tau}\left(\frac{x_i-\bar{x}}{\sigma_x}\right)\left(\frac{y_{i+\tau}-\bar{y}}{\sigma_y}\right) \qquad (1)$$

where $\bar{x}$ and σ_x denote mean and variance, while τ is the time lag. MSC or simply coherence is the cross-spectral density

function S_{xy}, which is simply derived via the fast Fourier transform (FFT) of (1), normalized by their individual autospectral density functions. However, due to finite size of neural data, one is forced to estimate the true spectrum, known as periodogram, using smoothing techniques (i.e., Welch's method). Thus, MSC is calculated as

$$\gamma_{xy}(f) = \frac{|\langle S_{xy}(f)\rangle|^2}{|\langle S_{xx}(f)\rangle|\,|\langle S_{yy}(f)\rangle|} \tag{2}$$

where $\langle\cdot\rangle$ indicates window averaging (a nonoverlapping Hamming window of 1024 samples length is used). The estimated MSC for a given frequency f ranges between 0 (no coupling) and 1 (maximum linear interdependence).

An alternative evaluation of the MSC, conventionally named autoregressive (AR) coherence (AR-COH), involves a bivariate AR process to model the analyzed times series [21]. For $n \in \{1,\ldots,N\}$, let $\mathbf{z}_n = [x_n\ y_n]^{\mathrm{T}}$, with the convention that $^{\mathrm{T}}$ denotes transposition. We consider the p-order AR process given by $\sum_{r=0}^{p} \mathbf{A}_r \mathbf{z}_{n-r} = \mathbf{e}_n$, where $\mathbf{A}_0$ is the identity matrix and the entries of all other $\mathbf{A}_r$ matrices are real valued. As usual, we assume null initial conditions. The Gaussian noise $\mathbf{e}_n$ is zero mean and for all integers k, $E[\mathbf{e}_t \mathbf{e}_{t-k}^{\mathrm{T}}] = \delta_{k,0}\Sigma$, where $E[\cdot]$ denotes the expectation operator and $\delta_{\cdot,\cdot}$ is the Kronecker operator. Furthermore, the spectral matrix can be factored as

$$\begin{bmatrix} S_{xx}(f) & S_{xy}(f) \\ S_{yx}(f) & S_{yy}(f) \end{bmatrix} = \mathbf{H}(f)\Sigma\mathbf{H}^*(f),$$

where $\mathbf{H}(f) = \left(\sum_{r=0}^{p} \mathbf{A}_r \exp(-2\pi j r f)\right)^{-1}$ with $j = \sqrt{-1}$, and $\mathbf{H}^*(f)$ is the conjugate transpose of $\mathbf{H}(f)$ [21]. AR-COH is computed with formula $|S_{xy}(f)|^2 / (S_{xx}(f)S_{yy}(f))$.

Given the measurements $x_1^N = x_1,\ldots,x_N$ and $y_1^N = y_1,\ldots,y_N$, we can resort to well-known algorithms for fitting a bivariate AR model. The algorithm of Whittle–Wiggins–Robinson (W2R) [22], [23] has the advantage that the stability of the estimated AR model is guaranteed. In our experiments, we utilized the algorithms W2R and ARFIT [24], [25]. As the AR-COH computed values were similar for the two estimation methods, we report here only the results obtained with W2R. The optimal model order was chosen from the predefined set $\{1,\ldots,50\}$ by applying the MDL criterion $\hat{p} = \operatorname{argmin}\left[\ln|\,\Sigma_p\,| + 4p(\ln N/N)\right]$, where $|\,\Sigma_p\,|$ is the determinant of the covariance matrix for the vector of residuals.

Once the AR coefficients are estimated, not only AR-COH can be easily computed, but also the feedback measures introduced by Granger [26] and Geweke [27] can be evaluated without difficulties [21]. The modest results obtained in [28] when employing the Geweke approach discourage us to consider it here.

D. An MDL Measure for Interchannel Coupling

The dependence between time series is recast to reflect the predictability of each of the two time series from the other, and the method can be applied for measuring the coupling between band-limited signals [7]. We are interested in evaluating the coupling between $\tilde{x}_1^N$ and $\tilde{y}_1^N$, where $\tilde{x}_1^N$ and $\tilde{y}_1^N$ are obtained after filtering x_1^N and y_1^N with a bandpass filter whose frequency range is $[\omega_{\inf}, \omega_{\sup}]$. The MDL principle claims the best model to be the one that leads to the shortest possible code length for the available measurements. Let the coded sample at instant t be $\tilde{y}_t$, $1 \le t \le N$. Using the hypothesis that $\tilde{y}_1^N = \tilde{y}_1,\ldots\tilde{y}_N$ must be transmitted from an encoder to a decoder, we apply the following methodology based on the results from [7].

1) First Coding Scenario: For an arbitrary prediction order $k \le k_{\max}$, we compute the predicted value $\hat{y}_t$ for $\tilde{y}_t$ based on the past samples $\tilde{y}_1^{t-1}$:$\hat{y}_t = \sum_{i=1}^{k} f_i\,\tilde{y}_{t-i}$. Let $\varepsilon_t = \tilde{y}_t - \hat{y}_t$ be the prediction error and $E[\varepsilon_t^2] = \varsigma_k^2$. The parameters f_i are chosen such as to minimize ς_k^2, and after quantization, they are sent to the decoder as side information. The prediction errors ε_t, $1 \le t \le N$, are also sent to the decoder and the asymptotic expression of the code length for $\tilde{y}_1^N$ is $(N/2)\ln\varsigma_k^2 + ((k+1)/2)\ln N$. We select the prediction order $k^* \in \{0,\ldots,k_{\max}\}$ so that the code length is minimized. After dividing by N, the aforementioned expression becomes $L(\tilde{y}_t|\tilde{y}_1^{t-1}) = (1/2)\ln\varsigma_{k^*}^2 + ((k^*+1)/2)(\ln N/N)$ [7].

2) Second Coding Scenario: Assuming the decoder has complete knowledge on the past and the present of $\tilde{x}$, the current value of $\tilde{y}$ can be predicted as $\hat{y}_t = \sum_{i=1}^{k^*} g_i\,\tilde{y}_{t-i} + \sum_{i=0}^{\ell} h_i\,\tilde{x}_{t-i}$, where $\ell \in \{0,\ldots,k^*-1\}$. The number of samples from the past of the $\tilde{y}$ and $\tilde{x}$ processes used in the linear regression depends on k^* that was determined in the previous step. For each possible value of ℓ, the parameters g_i and h_i are estimated from the available measurements such that to minimize the variance $\varsigma_{k^*,\ell}^2$ of the prediction errors. Then, the structure parameter ℓ^* is chosen to minimize the asymptotic code length. The expression of the code length is given by $L(\tilde{y}_t|\tilde{y}_1^{t-1},\tilde{x}_1^t) = (1/2)\ln\varsigma_{k^*,l^*}^2 + ((k^*+l^*+1)/2)(\ln N/N)$ [7]. The savings in code length of $\tilde{y}_1^N$ due to the knowledge on $\tilde{x}_1^N$ is a measure of dependence between the two processes that it is grounded in the MDL principle [7]. Based on this observation, we define $\mu_{\tilde{x}\to\tilde{y}} = L(\tilde{y}_t\,|\,\tilde{y}_1^{t-1}) - L(\tilde{y}_t\,|\,\tilde{y}_1^{t-1},\tilde{x}_1^t)$, and in the same way, $\mu_{\tilde{y}\to\tilde{x}} = L(\tilde{x}_t\,|\,\tilde{x}_1^{t-1}) - L(\tilde{x}_t\,|\,\tilde{x}_1^{t-1},\tilde{y}_1^t)$. We further define the MDL coupling measure: $\mu_{\tilde{x},\tilde{y}} = (\mu_{\tilde{x}\to\tilde{y}} + \mu_{\tilde{y}\to\tilde{x}})/2$.

Solving the estimation problem in the first coding scenario is equivalent with estimating the coefficients of an AR model, where we apply the Levinson–Durbin algorithm [29]. In our implementation, the maximum prediction order depends on the frequency band and takes values between 2 and 48. The second coding scenario relies on estimating the coefficients of an ARX model for which we employ the *arx* Matlab function.

E. Phase-Locking Value (PLV)

One of the mostly used PS measures is the PLV approach. It assumes that two dynamic systems may have their phases synchronized even if their amplitudes are zero correlated [30]. The PS is defined as the locking of the phases associated to each signal, such as

$$|\phi_x(t) - \phi_y(t)| = \text{const.} \tag{3}$$

In order to estimate the instantaneous phase of our signal, we transform it using the Hilbert transform (HT), whereby the

analytical signal $H(t)$ is computed as

$$H(t) = x(t) + i\tilde{x}(t) \tag{4}$$

where $\tilde{x}(t)$ is the HT of $x(t)$, defined as

$$\tilde{x}(t) = \frac{1}{\pi}\mathrm{PV}\int_{-\infty}^{\infty}\frac{x(t')}{t-t'}dt' \tag{5}$$

where PV denotes the Gauchy principal value.

The analytical signal phase is defined as

$$\phi(t) = \arctan\frac{\tilde{x}(t)}{x(t)}. \tag{6}$$

Therefore, for the two signals $x(t)$, $y(t)$ of equal time length with instantaneous phases $\phi_x(t), \phi_y(t)$, respectively, the PLV bivariate metric is defined as

$$\mathrm{PLV} = \left|\frac{1}{N}\sum_{j=0}^{N-1} e^{i(\phi_X(j\Delta t)-\phi_Y(j\Delta t))}\right| \tag{7}$$

where Δt is the sampling period and N is the sample number of each signal. PLV takes values within the [0,1] space, where 1 indicates perfect PS and 0 indicates lack of synchronization.

F. Robust State–Space GS Method (RS)

Alternatively, one may measure how neighborhoods (i.e., recurrences) in one attractor maps into the other. This idea turned out to be the most robust and reliable way of assessing the extent of GS [12], [13]. First, we reconstruct delay vectors [31] out of our time series; $x_n = (x_n, \ldots, x_{n-(m-1)\tau})$ and $y_n = (y_n, \ldots, y_{n-(m-1)\tau})$, where $n = 1,\ldots, N$, and m, τ are the embedding dimension and time lag, respectively. Let $r_{n,j}$ and $s_{n,j}$, $j = 1,\ldots, k$, denote the time indices of the k nearest neighbors of x_n and y_n, respectively. For each x_n, the mean squared Euclidean distance to its k neighbors is defined as

$$R_n^{(k)}(X) = \frac{1}{k}\sum_{j=1}^{k}(x_n - x_{r_{n,j}})^2 \tag{8}$$

and the Y-conditioned squared mean Euclidean distance $R_n^{(k)}(X\,|Y)$ is defined by replacing the nearest neighbors by the equal time partners of the closest neighbors of y_n.

If the set of reconstructed vectors (point cloud x_n) has an average squared radius $R(X) = (1/N)\sum_{n=1}^{N} R_n^{(N-1)}(X)$, then $R_n^{(k)}(X\,|Y) \approx R_n^{(k)}(X) \ll R(X)$ if the systems are strongly correlated, while $R_n^{(k)}(X\,|Y) \approx R(X) \gg R_n^{(k)}(X)$ if they are independent. Hence, an interdependence measure is defined as [12]

$$S^{(k)}(X\,|Y) = \frac{1}{N}\sum_{n=1}^{N}\frac{R_n^{(k)}(X)}{R_n^{(k)}(X\,|Y)}. \tag{9}$$

Since $R_n^{(k)}(X\,|Y) \gg R_n^{(k)}(X)$ by construction, it is clear that S ranges between 0 (indicating independence) and 1 (indicating maximum synchronization). Another normalized and more robust version of S maybe defined as in [13] and is the one actually used in this study:

$$N^{(k)}(X\,|Y) = \frac{1}{N}\sum_{n=1}^{N}\frac{R_n(X) - R_n^{(k)}(X\,|Y)}{R_n(X)}. \tag{10}$$

In the present study, RS was computed with the following parameter settings: $\tau = 20$; $m = 10$; $w_1 = 200$ samples (Theiler correction for autocorrelation effects [32]); $k = 10$.

G. Synchronization Likelihood (SL)

Finally, the last measure (SL) used is an unbiased normalized synchronization estimator closely related to the previous idea, which represents a normalized version of mutual information [14]. Supposing that x_n, x_v and y_n, y_v be the time delay vectors, SL actually expresses the chance that if the distance between x_n and x_v is very small, the distance between the corresponding vectors y_n and y_v in the state–space will also be very small. For this, we need a small critical distance ε_x, such that when the distance between x_n and x_v is smaller than ε_x, x will be considered to be in the same state at times n and v. The term ε_x is chosen such that the likelihood of two randomly chosen vectors from x (or y) will be closer than ε_x (or ε_y) equals a small fixed number p_{ref}. The term p_{ref} is the same for x and y, but ε_x need not be equal to ε_y. Now, SL between x and y at time n is defined as follows:

$$\mathrm{SL}_n = \frac{1}{N'}\sum_{\substack{v=1 \\ w_1<|n-v|<w_2}}^{N}\theta(\varepsilon_{y,n} - \|y_n - y_v\|)\theta(\varepsilon_{x,n} - \|x_n - x_v\|). \tag{11}$$

Here, $N' = 2(w_2 - w_1 - 1)p_{\mathrm{ref}}$, $\|\cdot\|$is the Euclidean distance, and θ is the Heaviside step function, $\theta(x) = 0$ if $x \leq 0$ and $\theta(x) = 1$ otherwise. The window of size w_1 implements the Theiler correction for autocorrelation effects and that of size w_2 is a window that sharpens the time resolution of the synchronization measure; window sizes are chosen such that $w_1 \ll w_2 \ll N$ [32]. When no synchronization exists between x and y, SL_n is equal to the likelihood that random vectors y_n and y_v are closer than ε_y; thus, $\mathrm{SL}_n = p_{\mathrm{ref}}$. In the case of complete synchronization, $\mathrm{SL}_n = 1$. Intermediate coupling is reflected by $p_{\mathrm{ref}} < \mathrm{SL}_n < 1$. Finally, SL is defined as the time average of the SL_n values. In the present study, SL was computed with the following parameter settings: $\tau = 20$; $m = 10$; $w_1 = 200$ samples; $w_2 = 500$ samples; $p_{\mathrm{ref}} = 0.05$.

III. Results

A. Testing the Nonlinear Methods Using Artificially Generated Data by Chaotic Oscillators Under Variable Noise

To check both the ability and robustness of the nonlinear techniques used to successfully detect nonlinear interdependencies under additive noise, we consider two classical coupled chaotic dynamical systems. The first model uses two coupled Rössler oscillators [18], configured to have PS, whereas the second uses a Lorenz system [19] nonlinearly driven by a Rössler oscillator with coupling coefficient that ensures GS.

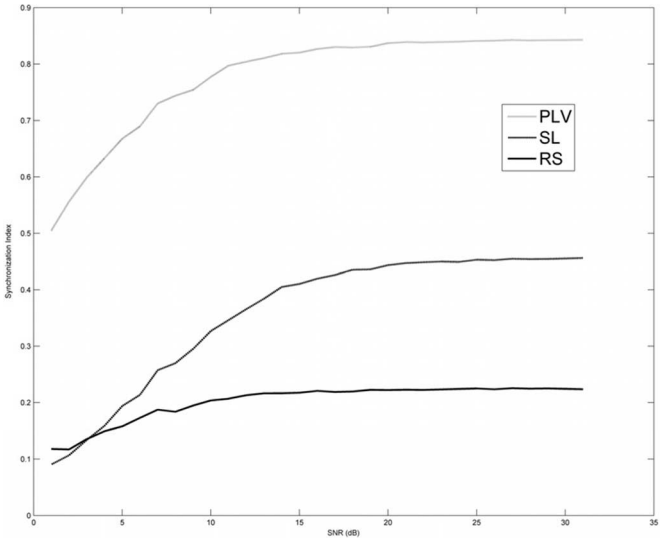

Fig. 1. SIs applied on two coupled Rössler oscillators, configured to have PS.

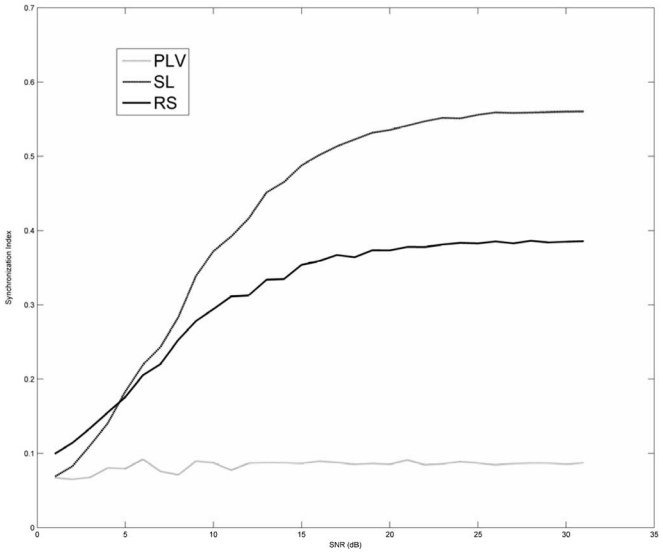

Fig. 2. SIs applied on a Lorenz system nonlinearly driven by a Rössler oscillator. The coupling coefficient used is set for general synchronization.

The synchronization indexes (SIs) versus additive noise SNRs are plotted in Figs. 1 and 2. In the first case (see Fig. 1), PLV obviously performs better, since it is itself a PS capturing measure. SL underestimates the true synchronization, whereas RS totally fails, since it is a purely GS measure. In the same way, PLV fails in the second case (see Fig. 2), whereas SL and RS are performing much better as GS capturing measures. More specifically, RS is found to be more robust than SL (the detected RS SI varies less than the SL case) when additive noise is introduced.

B. Nonlinear Coupling Detection Ability: Testing Using Surrogates

To demonstrate the existence of nonlinear structures and justify the use of nonlinear tools in the analysis of the real EEG signals under investigation, bivariate surrogate data testing was used [33]. The surrogating procedure preserves both the autocorrelation of the signals and their linear cross-correlation, but destroys the nonlinear individual structure of the signals as well as their nonlinear interdependence, if any [34]. More specifically, we consider 30 surrogate time series pairs that maintain their linear cross-correlation as well as their linear autocorrelation up to a time lag and are otherwise random. Next, the null hypothesis (H_0) that the original data only reflects linear interdependencies is tested. To test H_0, the outcome of a nonlinear synchronization measure applied to the original (actual) data is compared to the outcomes of the measure applied to the 30 surrogate bivariate time series. This hypothesis is tested by computing the Z-score value, which expresses the number of standard deviations (SDs) each SI is away from the mean SIs of the surrogate data.

$$Z = \frac{(\mathrm{SI} - \mathrm{SI}_{\mathrm{surrogates}})}{\overline{\mathrm{SD}}_{\mathrm{surrogates}}} \tag{12}$$

If $Z > 1.96$ (one-sided test), then H_0 is rejected at the 95% level of confidence, implying that the value of the original and the mean of the set of surrogate time series is significantly different. The results of surrogate data testing using PLV and RS are calculated for all 20 controls (see Table I) and epileptic (see Table II) children, during the fractal observation test. The median, minimum, and maximum Z-score values are tabulated for selected channel pairs focusing on brain regions that cover different functional lobes of the working brain in gamma2 band (40–90 Hz). SL was not included since the findings were similar to those of RS (both are representatives of the GS case), and the latter was found to be more robust under additive noise as shown in the previous section.

In all lobes tested using the PLV method, the Z-scores range from lower to higher values than 1.96. Consequently, there is statistical evidence in a subgroup of subjects that the interdependence cannot be fully described by a linear stochastic model. Comparable results were obtained with the RS index as well. At the same time, there are also cases where the Z-score is less than the critical value of 1.96, meaning that there are strong linear interdependencies in the actual datasets. In the 160 (20 subjects, 8 lobes) epochs tabulated, nonlinearity was

TABLE I
SYNCHRONIZATION Z-SCORES IN NORMAL SUBJECTS (ORIGINAL VERSUS SURROGATE DATASETS)

Brain Lobe	PLV Z-score		RS Z-score	
	median (min-max)	subjects with Z>1.96	median (min-max)	subjects with Z>1.96
FP1-F3	1.78 (0.13-4.16)	10	1.38 (0.01-6.22)	8
FP2-F4	2.11 (0.05-6.41)	11	1.72 (0.08-4.35)	10
T3-TP7	0.86 (0.08-4.43)	4	1.47 (0.28-4.51)	8
T4-TP8	1.56 (0.01-3.28)	5	1.32 (0.16-5.36)	9
CP3-P3	0.90 (0.09-2.70)	3	0.94 (0.04-3.96)	8
CP4-P4	1.15 (0.12-2.53)	1	1.54 (0.11-2.74)	6
7P4-O2	0.85 (0.03-5.15)	3	1.48 (0.30-7.58)	7
P3-O1	0.83 (0.01-3.33)	5	1.98 (0.72-4.59)	11

TABLE II
SYNCHRONIZATION Z-SCORES IN EPILEPTIC SUBJECTS (ORIGINAL VERSUS SURROGATE DATASETS)

Brain Lobe	PLV Z-score		RS Z-score	
	median (min-max)	subjects with Z>1.96	median (min-max)	subjects with Z>1.96
FP1-F3	1.06 (0.09-3.45)	5	1.16 (0.00-6.03)	6
FP2-F4	0.97 (0.09-2.82)	4	1.13 (0.02-3.34)	4
T3-TP7	1.02 (0.12-3.27)	4	1.06 (0.20-3.49)	6
T4-TP8	0.78 (0.01-2.93)	4	0.96 (0.13-3.65)	5
CP3-P3	0.85 (0.02-3.83)	2	1.12 (0.01-5.49)	3
CP4-P4	0.66 (0.03-3.98)	4	0.70 (0.03-3.37)	4
P4-O2	0.74 (0.06-2.17)	1	1.21 (0.10-3.79)	6
P3-O1	1.10 (0.14-2.58)	4	1.01 (0.05-3.52)	7

found in 26.25% and in 41.88% of the epochs listed in Table I using the PLV and the RS method, respectively. Similarly, in Table II, nonlinearity was found in 17.5% and in 25.63% of the epochs listed, using the PLV and the RS method, respectively. To maintain an experiment-wise α level of 0.05, the significance of the individual tests has to be Bonferroni corrected: $P = (0.05/160) = 0.0003125$. This corresponds with a Z-score larger than 3.42. With this Bonferroni correction, nonlinearity was found in 3.13% and in 10% of the epochs listed in Table I, using the PLV and the RS method, respectively. In Table II, nonlinearity was found in 1.88% and in 4.38% of the epochs listed, using the PLV and the RS method, respectively. Hence, one should use both linear and nonlinear measures. Such testing was performed only on the nonlinear synchronization measures, since linear measures are not expected to differentiate their values from the actual signal to the linear surrogates [28].

C. Actual EEG Data

Testing using surrogates suggested that real data should be analyzed using both linear and nonlinear methods. Hence, PLV and RS measures are performed on both "normal" and "mild-epileptic" band-filtered data (using a fourth degree zero-phase Butterworth filter). Averages over all possible channel couplings in each brain lobe and band are calculated (see Table III). Only those methods and the related bands/lobes that achieved significant differentiation using ANOVA ($p = 0.05$) statistics are tabulated. The terms θ, α_1, α_2, β, γ_1, and γ_2 denote theta (4–8 Hz), alpha1 (8–10 Hz), alpha2 (10–13 Hz), beta (13–30 Hz), gamma1 (30–40 Hz), and gamma2 (40–90 Hz) bands, respectively. The identified lobes are: OPR (O2-P4, O2-P8, P4-P8), OPL (O1-P3, O1-P7, P7-P3), CPL (C3-CP3, CP3-P3, P3-P7), TL (FT7-T3, T3-TP7, FT7-TP7), and FL (FP1-F7, FP1-F3, F7-F3), while $N > E$ denotes that synchronization in normal controls is greater than in epileptics in the specified band and brain region. In Table III, p-values along with mean and SDs of each SI of each group is tabulated.

The nonlinear methods (PLV and RS) do not identify any synchronization differences under the control task. During fractals

TABLE III
ACTUAL EEG DATA: LOBE-BAND SELECTION

Method	Test 1 (Control)	Test 2 (Fractals)
MSC	α_1: **OPL**$^{(N>E)}$, p:0.049 N:0.66±0.17, E:0.55±0.15	-
AR-COH	α_2: **OPL**$^{(N>E)}$, p:0.019 N:0.62±0.13, E:0.50±0.18	θ: **OPL**$^{(N>E)}$, p:0.033 N:0.68±0.13, E:0.54±0.23 α_1: **OPL**$^{(N>E)}$, p:0.017 N:0.66±0.10, E:0.54±0.18 α_1: **OPR**$^{(N>E)}$, p:0.009 N:0.61±0.11, E:0.49±0.16 γ_1: **OPR**$^{(N>E)}$, p:0.042 N:0.71±0.12, E:0.61±0.17
MDL	-	β: **OPR**$^{(N>E)}$, p:0.034 N:0.43±0.19, E:0.28±0.22 γ_2: **OPR**$^{(N>E)}$, p:0.002 N:0.34±0.22, E:0.14±0.16 γ_2: **TL**$^{(N>E)}$, p:0.034 N:0.38±0.30, E:0.19±0.25
PLV	-	γ_2: **OPL**$^{(N>E)}$, p:0.038 N:0.82±0.08, E:0.74±0.15 γ_2: **OPR**$^{(N>E)}$, p:0.022 N:0.80±0.09, E:0.72±0.14
RS	-	γ_2: **OPL**$^{(N>E)}$, p:0.025 N:0.68±0.09, E:0.58±0.17 γ_2: **OPR**$^{(N>E)}$, p:0.021 N:0.67±0.11, E:0.57±0.15

observation, PLV and RS consistently identified differences in both OPL and OPR for the gamma2 band. Similar differences were indicated by the MDL method but with a high variance within each population, rendering its results less confident. MSC was able to spot a weak coupling in a_1-OPL ($p > 0.04$) during the control task. AR-COH did identify the same region with increased significance, but in the neighboring α_2 band. In addition, AR-COH appears to be a more sensitive coherence method able to identify OPL and OPR differences during the visual task, even though at lower frequencies than their nonlinear counterparts. Probably, both sets of techniques identified parts of a broader activation pattern in OPL and OPR (both linear and nonlinear), but this should require more extensive validation.

To visualize the network topology of the results, graphs (see Fig. 3) were used to depict the average RS synchronization interdependences over all 20 subjects in each group. Each edge indicates the presence of strong interdependence (higher than a preselected threshold) between all possible pairs of channels. The threshold was kept constant for the visualization purposes of both the normal and epileptic groups. The "control" graph [see Fig. 3(a)] appears to exhibit a denser network compared to the "epileptic" one [see Fig. 3(b)]. Similar graph topology was achieved in the case of PLV as well.

IV. DISCUSSION

The PLV method applied on phase-synchronized oscillators obviously was the measure that performed better (see Fig. 1). SL and RS estimators were also able to identify the coupling, but underestimated it. However, on the second paradigm using

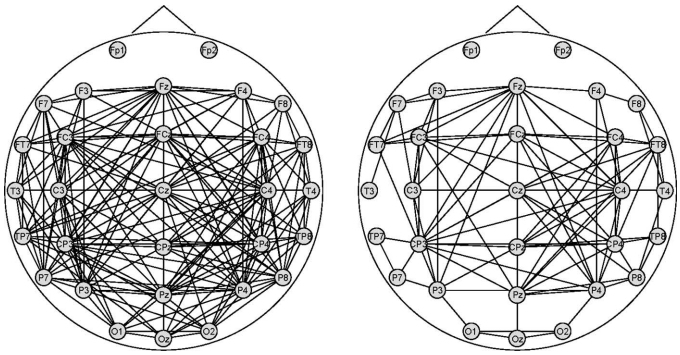

Fig. 3. Network of normal (left graph) (during the fractal observation task and fixed selected threshold) appears to have more interconnections (denser network) compared to the "epileptic" one (right graph). These disturbances are more prominent for the connections of the parieto–occipital lobes. Note that both graphs depict the averaged RS synchronization interdependences (gamma2 band) over all 20 subjects in each group.

the generally synchronized oscillators, all methods were able to perform well, except the PLV as expected, since the oscillator was optimized for GS (see Fig. 2). The different responses of SL and RS are due to normalization factors and do not imply that one outperforms the other. As a conclusion in a real case scenario, one should use both a PS measure (i.e., PLV) and one of the proposed GS measures (preferably RS), as well as linear tools since their underlined assumptions are different. The testing using surrogate datasets also testifies strong statistical evidence that the interdependence in the real EEG data can be partially described by a linear model. But at the same time, there also exists PS and GS nonlinear coupling. The fact that both the nonlinear methods (PLV and RS) were able to discriminate the actual EEG from the surrogates (linear representations) leads to the conclusion that the actual EEG data do contain significant nonlinear synchronization couplings. The results (see Table III) indicate that the PLV and RS methods accentuate gamma2 reactivity on the occipital brain lobes during the fractal simulation test. These findings may also be visualized and validated using graph topological plots (see Fig. 3). Apparently, in the case of epilepsy, significantly fewer edges are driven from the occipital and parietal channels (O1, O2, P3, P7, P4, P8) compared to the control case. Linear synchronization estimators accentuate reactivity in lower frequency bands, and they also support activations around the occipital regions. In all methods, the indicated differences during the fractal observation task are located in the regions of cortex responsible for vision (occipital), where visual stimuli are perceived. This reactivity is always lower in epileptic children indicating the ability of such methods to evaluate cortical dysfunction. This effect is unlikely to be attributed to drugs, since they are only administered at low dosages. Furthermore, if the presence of drugs was dominating, one would expect a rather diffused activation pattern across most of the brain lobes, especially in slower frequency bands, which was not observed.

Numerous studies have observed an increase in induced gamma band energy with increases in covert selective attention and visual perception [35]. Fractal observation involves both processing in the first cortical region (V1) and processing at higher levels, when each participant perceives primitive features (i.e., oriented contrast gradients) and even more complex patterns by combining inputs from lower levels, respectively [36]. Such an information flow has been extensively studied in the literature and is referred as bottom-up (B-U) binding [35], [37]. At the same time, a top-down (T-D) flow of information is also evident in gamma band, the function of which is less clear [35]. Anatomical studies have demonstrated the existence of massive connections from higher level areas, back to lower level areas and are believed to strongly affect neuronal function [38] and provide a way for high-level information to affect perception. The T-D flow is mostly related to attention processes, while each participant is setting context (knowing what to expect). The match between B-U and T-D information is also believed to be reflected in gamma-band activity [39].

V. Conclusion

Human response to the visual qualities of fractal images constitutes a novel test bed for visual perception studies. Such complex targets, also present in natural environments, together with advanced linear/nonlinear synchronization methodologies may be of future clinical use in evaluating cortical dysfunctions in cases where classical EEG evaluation methods fail. The use of bivariate surrogate data allows us to check that the actual interdependencies among lobe activations are not only linear but also nonlinear. In such case, nonlinear methods complete the whole picture as they allow the analysis of complex cortical interactions from different perspectives and complement the information provided by traditional linear tools. The results presented indicate a significant synchronization difference between normal controls and epileptics, mostly apparent in occipital–parietal lobes, during fractal observation tests. Nonlinear methods identified this difference in the higher frequency band of gamma2, whereas the linear ones identified the same regions but shifted toward lower frequencies. Additional validation of such results may support the presence of such a marker of cortical dysfunction in identifying mild epileptic cases. This would probably require a combination of methods in order to encapsulate both linear and nonlinear interdependencies.

References

[1] W. Singer, "Consciousness and the binding problem," *Ann. NY Acad. Sci.*, vol. 929, pp. 123–146, 2001.

[2] E. Basar, C. Basar-Eroglu, S. Karakas, and M. Schurmann, "Gamma, alpha, delta, and theta oscillations govern cognitive processes," *Int. J. Psychophysiol.*, vol. 39, pp. 241–248, 2001.

[3] A. P. Anokhin, W. Lutzenberger, and N. Birbaumer, "Spatiotemporal organization of brain dynamics and intelligence: An EEG study in adolescents," *Int. J. Psychophysiol.*, vol. 33, pp. 259–273, 1999.

[4] A. von Stein and J. Sarnthein, "Different frequencies for different scales of cortical integration: From local gamma to long range alpha theta synchronization," *Int. J. Psychophysiol.*, vol. 38, pp. 301–313, 2000.

[5] M. Ford, J. Goethe, and D. Dekker, "EEG coherence and power changes during a continuous movement task," *Int. J. Psychophysiol.*, vol. 4, pp. 99–110, 1986.

[6] S. Micheloyannis, V. Sakkalis, M. Vourkas, C. J. Stam, and P. G. Simos, "Cortical networks involved in mathematical thinking: Evidence from linear and non-linear cortical synchronization of electrical activity," *Neurosci. Lett.*, vol. 373, pp. 212–217, 2005.

[7] J. Rissanen and M. Wax, "Measures of mutual and causal dependence between two time series," *IEEE Trans. Inf. Theory*, vol. 33, no. 4, pp. 598–601, Jul. 1987.
[8] S. R. Butler and A. Glass, "Asymmetries in the electroencephalogram associated with cerebral dominance," *Electroencephalogr. Clin. Neurophysiol.*, vol. 36, no. 5, pp. 481–491, 1974.
[9] A. Pikovsky, M. Rosenblum, and J. Kurths, *Synchronization: A Universal Concept in Nonlinear Science*. Cambridge, U.K.: Cambridge Univ. Press, 2001.
[10] J. Lachaux, E. Rodriguez, J. Martinerie, and F. Varela, "Measuring phase synchrony in brain signals," *Human Brain Mapp.*, vol. 8, pp. 194–208, 1999.
[11] K. Matsumoto and I. Tsuda, "Calculation of information flow rate from mutual information," *J. Phys. A*, vol. 21, pp. 1405–1414, 1988.
[12] J. Arnhold, P. Grassberger, K. Lehnertz, and C. E. Elger, "A robust method for detecting interdependencies: Application to intracranially recorded EEG," *Phys. D*, vol. 134, pp. 419–430, 1999.
[13] R. Q. Quiroga, A. Kraskov, T. Kreuz, and P. Grassberger, "Performance of different synchronization measures in real data: A case study on electroencephalographic signals," *Phys. Rev. E*, vol. 65, pp. 041903-1–041903-14, 2002.
[14] C. J. Stam and B. W. van Dijk, "Synchronization likelihood: An unbiased measure of generalized synchronization in multivariate data sets," *Phys. D*, vol. 163, pp. 236–251, 2002.
[15] L. L. Bailet and W. R. Turk, "The impact of childhood epilepsy on neurocognitive and behavioral performance: A prospective longitudinal study," *Epilepsia*, vol. 41, no. 4, pp. 426–431, 2000.
[16] J. Williams, T. Phillips, M. L. Griebel, G. B. Sharp, B. Lange, T. Edgar, and P. Simpson, "Factors associated with academic achievement in children with controlled epilepsy," *Epilepsy Behav.*, vol. 2, pp. 217–223, 2001.
[17] P. Camfield and C. Camfield, "Epileptic syndromes in childhood: Clinical features, outcomes, and treatment," *Epilepsia*, vol. 43, no. 3, pp. 27–32, 2002.
[18] A. Hramov and A. Koronovskii, "Intermittent generalized synchronization in unidirectionally coupled chaotic oscillators," *Europhys. Lett.*, vol. 70, no. 2, pp. 169–175, 2005.
[19] A. Hramov and A. Koronovskii, "Generalized synchronization: A modified system approach," *Phys. Rev. E*, vol. 71, pp. 067201-1–067201-4, 2005.
[20] V. O. Mitina and F. D. Abraham, "The use of fractals for the study of the psychology of perception," *Int. J. Mod. Phys. C*, vol. 14, pp. 1047–1060, 2003.
[21] A. Brovelli, M. Ding, A. Ledberg, Y. Chen, R. Nakamura, and S. L. Bressler, "Beta oscillations in a large-scale sensorimotor cortical network: Directional influences revealed by Granger causality," *Proc. Nat. Acad. Sci. USA*, vol. 101, no. 26, pp. 9849–9854, 2004.
[22] P. Whittle, "On the fitting of multivariate autoregressions and the approximate canonical factorization of a spectral density matrix," *Biometrika*, vol. 50, pp. 129–134, 1963.
[23] R. Wiggins and E. Robinson, "Recursive solution to the multichannel filtering problem," *J. Geophys. Res.*, vol. 70, pp. 1885–1891, 1966.
[24] T. Schneider and A. Neumaier, "Algorithm 808: ARFIT—A Matlab package for the estimation of parameters and eigenmodes of multivariate autoregressive models," *ACM Trans. Math. Softw.*, vol. 27, no. 1, pp. 58–65, 2001.
[25] ARFIT. (2007, Oct. 12). Fitting multivariate autoregressive models [Online]. Available: http://www.gps.caltech.edu/∼tapio/arfit/
[26] C. W. J. Granger, "Investigating causal relations by econometric models and cross-spectral methods," *Econometrica*, vol. 37, no. 3, pp. 424–438, 1969.
[27] J. Geweke, "Measurement of linear dependence and feedback between multiple time series," *J. Amer. Statist. Assoc.*, vol. 77, no. 378, pp. 304–313, 1982.
[28] V. Sakkalis, C. D. Giurcăneanu, P. Xanthopoulos, M. Zervakis, Y. Yang, and S. Micheloyannis, "Assessment of linear and non-linear EEG synchronization measures for evaluating mild epileptic signal patterns," presented at the Proc. Inf. Technol. Appl. Biomed. (ITAB), Ioannina, Greece, Oct. 26–28, 2006.
[29] D. G. Manolakis, V. K. Ingle, and S. M. Kogon, *Statistical and Adaptive Signal Processing*. Norwood, MA: Artech House, 2005.
[30] F. Mormann, K. Lehnertz, P. David, and C. Elger, "Mean phase coherence as a measure for phase synchronization and its application to the EEG of epilepsy patients," *Phys. D*, vol. 144, pp. 358–369, 2000.
[31] F. Takens, D. A. Rand, and L. S. Young, "Detecting strange attractors in turbulence," *Dyn. Syst. Turbulence, Lect. Notes Math.*, vol. 898, pp. 366–381, 1981.
[32] J. Theiler, "Spurious dimension from correlation algorithms applied to limited time-series data," *Phys. Rev. A*, vol. 34, no. 3, pp. 2427–2432, 1986.
[33] R. G. Andrzejak, A. Kraskov, H. Stogbauer, F. Mormann, and T. Kreuz, "Bivariate surrogate techniques: Necessity, strengths, and caveats," *Phys. Rev. E*, vol. 68, no. 6, pp. 066202-1–066202-5, 2003.
[34] T. Schreiber and A. Schmitz, "Surrogate time series," *Phys. D*, vol. 142, no. 3/4, pp. 346–382, 2000.
[35] A. Posada, E. Hugues, P. Vianin, N. Franck, and J. Kilner, "Augmentation of induced visual gamma activity by increased task complexity," *Eur. J. Neurosci.*, vol. 18, pp. 1–6, 2003.
[36] R. C. Reid, "Divergence and reconvergence: Multielectrode analysis of feedforward connections in the visual system," *Prog. Brain Res.*, vol. 130, pp. 141–154, 2001.
[37] C. Tallon-Baudry and O. Bertrand, "Oscillatory gamma activity in humans and its role in object representation," *Trends Cogn. Sci.*, vol. 3, pp. 151–162, 1999.
[38] P. A. Salin and J. Bullier, "Corticocortical connections in the visual system: Structure and function," *Psychol. Bull.*, vol. 75, pp. 107–154, 1995.
[39] C. S. Herrmann, M. H. Munk, and A. K. Engel, "Cognitive functions of gamma-band activity: memory match and utilization," *Trends Cogn. Sci.*, vol. 8, no. 8, pp. 347–355, 2004.

Vangelis Sakkalis received the Master's degree in biomedical engineering from the Imperial College of Science, Technology and Medicine, London, U.K., in 2000, and the Ph.D. degree in electronics and computer engineering from the Technical University of Crete, Chania, Greece, in 2006.

He is currently a member of the Institute of Computer Science, Foundation for Research and Technology (ICS–FORTH), Heraklion, Greece. He is also with the Department of Electronic and Computer Engineering, Technical University of Crete, Chania, Greece. He was engaged in research on biomedical engineering, atomic molecular physics, optoelectronics, and laser. His current research interests include biomedical signal and image analysis, visualization, classification algorithms, biostatistics, and biomedical informatics.

Ciprian Doru Giurcăneanu (S'98–M'02) received the Ph.D. degree (with honors) in signal processing from the Department of Information Technology, Tampere University of Technology, Tampere, Finland, in 2001.

From 1993 to 1997, he was a Junior Assistant at "Politehnica" University of Bucharest, Bucharest, Romania. Since 1997, he has been with Tampere University of Technology. He is currently a Research Fellow with the Academy of Finland, Helsinki, Finland. His current research interests include stochastic complexity and its applications.

Dr. Giurcăneanu is the Chair of the IEEE Finland joint Signal Processing and Circuits and Systems Chapter since 2006.

Petros Xanthopoulos received the Dipl. Eng. degree in electronics and computer engineering from the Electronics and Computer Engineering Department, Technical University of Crete, Chania, Greece, in 2005. He is currently working toward the Ph.D. degree in the Industrial and Systems Engineering Department, University of Florida, Gainesville.

He is currently a Research Assistant at the Center for Applied Optimization, University of Florida. His current research interests include optimization, biomedical signal processing, epileptic seizure detection, and data mining.

Michalis E. Zervakis (S'86–M'89) received the Ph.D. degree in electronics engineering from the Department of Electrical Engineering, University of Toronto, Toronto, ON, Canada, in 1990.

From September 1990 to December 1994, he was an Assistant Professor at the University of Minnesota-Duluth, Duluth. In January 1995, he joined the Technical University of Crete, Chania, Greece, where he is currently a Professor in the Department of Electronic and Computer Engineering, and also the Director of the Digital Image and Signal Processing Laboratory (DISPLAY), where he is engaged in research on modern aspects of signal processing, including estimation and constrained optimization, multichannel and multiband signal processing, wavelet analysis for data/image processing and compression, neural networks and fuzzy logic with applications in biomedical data analysis, imaging systems, and integrated automation systems, DSP-based real-time implementation.

Prof. Zervakis was an Associate Editor of the "IEEE TRANSACTIONS ON SIGNAL PROCESSING" from 1994 to 1996.

Vassilis Tsiaras received the B.S. degree in mathematics from Aristotle University, Thessaloniki, Greece, in 1990, and the M.S. degree in mathematics with computation from Queen Mary and Westfield College, London, U.K., in 1992. He is currently working toward the Ph.D. degree in computer science from the University of Crete, Heraklion, Greece.

His current research interests include graph visualization, complex networks, and graphical models for time series.

Yinghua Yang received the B.S. degree in electrical engineering from Shanghai Jiao Tong University, Shanghai, China, in 2000, and the M.S. degree in signal processing from Tampere University of Technology, Tampere, Finland, in 2006.

He is currently a Senior Design Engineer in Nokia Devices R&D, Tampere, Finland. His current research interests include data compression and signal processing.

Eleni Karakonstantaki was born in Venice, Italy. She studied psychology from the University of Crete, Rethymnon, Greece. She is working toward the Ph.D. degree on the neuropsychology of arithmetic disabilities of school-age children and their rehabilitation from the Medical School of Crete, Heraklion, Greece.

She is currently with the Clinical Neurophysiological Laboratory, Medical School of Crete, where she is engaged in clinical evaluation with electroencephalographic signal analysis and performing neuropsychological assessments to investigate the cognitive processes in normal and disturbed children. Her current research interest include learning disabilities such as language difficulties and dyscalculia.

Sifis Micheloyannis was born in Crete, Greece. He received the M.D. degree in neurology from the University of Crete-Medical Division, Crete, Greece, in 1980.

He was engaged in study of medicine at Athens University. He is with the Clinical Neurophysiology Laboratory (L. Widen), Faculty of Medicine, University of Crete, Heraklion, Greece, where he is a currently a Clinical Neurophysiologist. He was with the university hospitals in several European countries for more than ten years. He is engaged in clinical child neurology. His current research interests include the study of cognitive processes using bioelectrical signals, ongoing electroencephalographic activity at rest, and comparisons with the activity during cognitive processes. The methods he uses are based on "classical" spectral analysis, as well as nonlinear and graph theoretical tools.